Journal of Proteomics 310 (2025) 105339

Contents lists available at ScienceDirect

Journal of Proteomics

journal homepage: www.elsevier.com/locate/jprot

Proteomic analysis of the human amniotic mesenchymal stromal cell secretome by integrated approaches via filter-aided sample preparation

Alexandra Muntiu [a,1], Andrea Papait [b,c,1], Federica Vincenzoni [c,d], Diana Valeria Rossetti [a], Pietro Romele [e], Anna Cargnoni [e], Antonietta Silini [e], Ornella Parolini [b,c,2], Claudia Desiderio [a,*,2]

[a] Istituto di Scienze e Tecnologie Chimiche (SCITEC) "Giulio Natta", Consiglio Nazionale delle Ricerche, Rome, Italy
[b] Department of Life Science and Public Health, Università Cattolica del Sacro Cuore, Rome, Italy
[c] Fondazione Policlinico Universitario "Agostino Gemelli" Istituto di Ricovero e Cura a Carattere Scientifico, IRCCS, Rome, Italy
[d] Dipartimento di Scienze Biotecnologiche di Base, Cliniche Intensivologiche e Perioperatorie, Università Cattolica del Sacro Cuore, Rome, Italy
[e] Centro di Ricerca E. Menni, Fondazione Poliambulanza Istituto Ospedaliero, Brescia, Italy

ARTICLE INFO

Keywords:
Proteomics
Peptidomics
Secretome
Human amniotic mesenchymal stromal cells
Filter-aided sample preparation

ABSTRACT

The immunomodulatory, anti-inflammatory and regenerative properties of the human amniotic mesenchymal stromal cells (hAMSCs) secretome are acknowledged but the understanding of the specific bioactive components remains incomplete. To address these limitations, the present investigation aimed to profile the proteins and peptides content of the hAMSC secretome through sample pretreatment and fractionation on 10 kDa molecular cut-off FASP (Filter Aided Sample Preparation) device and LC-MS analysis. The filter retained protein fraction underwent trypsin digestion, while the unretained was collected unchanged for intact small proteins and peptides analysis. This combined approach (C-FASP) collects in a single step two complementary fractions, advantageously saving sample volume and time of analysis. The bottom-up analysis of the C-FASP proteins fraction >10 kDa confirmed our previous findings, establishing a set of proteins consistently characterizing the hAMSC secretome. The analysis of the fraction <10 kDa, never been investigated to our knowledge, identified peptide fragments of thymosin beta 4 and beta 10, collagen alpha 1 chains I and III, alpha-enolase, and glyceraldehyde-3-phosphate dehydrogenase, involved in wound healing, anti-inflammatory response, tissue repair and regeneration, key biological activities of the secretome. C-FASP provided a comprehensive molecular profile of the hAMSC secretome offering new insights for enhanced therapeutic applications in regenerative medicine.

Significance: In this investigation we originally present the comprehensive proteomic investigation of the human amniotic mesenchymal stromal cell secretome by combining the analysis of the proteome and of the peptidome following sample pretreatment and fractionation by Filter Aided Sample Preparation (FASP) with 10 kDa molecular cut-off in coupling with LC-MS analysis. The proteome fraction retained by FASP filter was analyzed after enzymatic digestion, while the unretained fraction, below 10 kDa molecular mass, was analyzed unchanged in its intact form. This dual approach provides novel insights, previously unexplored, into the molecular components potentially responsible for the immunomodulatory and anti-inflammatory properties of the hAMSC secretome. These findings could significantly enhance the therapeutic potential of hAMSCs in regenerative medicine.

1. Introduction

The secretome of human amniotic mesenchymal stromal cells (hAMSCs) is renowned for its immunomodulatory, anti-inflammatory, and regenerative properties [1]. However, our understanding of the specific contributing factors remains incomplete [2]. The unique characteristics of hAMSCs are attributed to the secretion of several bioactive molecules, including growth factors, extracellular matrix proteins, remodeling enzymes, pro-inflammatory and anti-inflammatory cytokines, chemokines, and angiogenic factors [1–5]. Despite their

* Corresponding author.
E-mail address: claudia.desiderio@cnr.it (C. Desiderio).
[1] These authors contributed equally to the work.
[2] These authors contributed equally to the work and shared co-senior authorship.

https://doi.org/10.1016/j.jprot.2024.105339
Received 11 June 2024; Received in revised form 18 October 2024; Accepted 21 October 2024
Available online 22 October 2024

acknowledged significance and previous proteomic investigations [6–9], studies focusing on the small proteins and peptides composition of the hAMSCs secretome have been not reported still, to the best of our knowledge, creating a gap in deciphering its complete proteomic profile.

Our study addresses this gap by integrating proteomic and peptidomic characterization of the hAMSCs secretome applying different analytical approaches to the proteome fractions obtained by Field Aided Sample Preparation (FASP) with 10 kDa filter molecular cut-off.

FASP is one commonly employed protocol for digesting protein mixtures [10,11]. This method utilizes molecular mass cut-off filter membranes for purifying, digesting, and concentrating the retained protein fraction, thereby enhancing analysis sensitivity. However, it simultaneously discards the protein fraction not retained by the filter. In a prior investigation [9], we successfully applied FASP to characterize the hAMSCs secretome's supernatant proteome fraction >10 kDa after digestion, potentially missing relevant information on small proteins and peptides in the fraction not retained by the filter.

A previous study [12] suggested that molecules influencing the immunomodulatory effect of the hAMSCs secretome reside in molecular mass fractions below 3 kDa and above 100 kDa. Notably, the fraction below 3 kDa was able to significantly inhibit T cell proliferation, prompting an extension of the proteomic investigation to a lower molecular mass range, an area that to the best of our knowledge is largely unexplored.

In pursuit of a comprehensive proteomic characterization of the hAMSCs secretome across the entire molecular mass range, we applied a modified FASP protocol. This modification enables the analysis of both the proteome and the peptidome of the hAMSCs secretome in one step. We termed this approach Combined-FASP (C-FASP) because it combines the preparation of the same sample aliquot for both proteomic analysis of the retained fraction using a bottom-up approach with trypsin digestion, and direct analysis of the unretained fraction for small proteins and peptides in their intact form using a top-down approach. Moreover, the two fractions can be advantageously analyzed under the same LC-MS operative conditions because, after enzymatic digestion of the FASP supernatant, they share a similar molecular mass range, either characterized by proteolytic protein fragment (FASP filter retained fraction) or by naturally occurring peptides and small proteins (FASP filter unretained fraction). Therefore, C-FASP, by processing the same aliquot for both proteomic and peptidomic analyses, and eliminating the need for column changing and preconditioning, significantly reduces the total analysis time and conserves sample volume. Additionally, it enables direct qualitative and quantitative comparison of the resulting proteo-peptidomic data, facilitating their integration in a single step. The LC-MS analysis across four hAMSCs secretome batches by C-FASP is illustrated in separate paragraphs describing the results of the proteome fractions analyzed with the proper analytical approach. It is noteworthy that, unlike the broad proteomic goal of maximizing protein identifications, our study aimed to identify the protein and peptide components that consistently characterize the hAMSC secretome and its biological activities. Consequently, the data were processed with stringent filters following the Human Proteome Project (HPP) Mass Spectrometry Data Interpretation Guidelines [13], to ensure high-confidence identifications, even though this approach significantly reduced the number of identified proteins and peptides.

2. Materials and methods

2.1. Preparation of hAMSCs secretome

Mesenchymal stromal cells from the amniotic membrane (hAMSC) were obtained as previously reported [14]. The study adhered to the principles of the Declaration of Helsinki, and informed consent was obtained following the guidelines outlined by the Brescia Provincial Ethics Committee (number NP 2243, 19/01/2016). hAMSCs were phenotypically characterized after isolation [14] and met the minimal criteria required for mesenchymal stromal cells (MSCs) [15,16]. hAMSCs at passage 1 were cultured for 5 days in 24-well plates (Corning, NY, USA) at a density of 5×10^5 cells/well in 0.5 mL of DMEM-F12 medium (Sigma-Aldrich) without serum, supplemented with 2 mM L-glutamine (Sigma-Aldrich) and 1 % P/S, as described [14]. After culture, the cell conditioned medium (referred to as the hAMSCs secretome), was collected, centrifuged, filtered through a 0.2 μm sterile filter (Sartorius Stedim, Florence, Italy), and stored at −80 °C. A 2500 μL aliquot was lyophilized, as previously reported. Each 2500 μL aliquot of secretome was obtained from 2.5 × 10^6 cells [17]. Four distinct pools (Pools I-IV) of hAMSCs secretomes were generated for this study. Pools I, II, and IV each consisted of secretomes from 4 different donors, and Pool III consisted of secretomes from 7 donors. Each pool was validated for immunomodulatory activity, as detailed in [17].

2.2. Secretome sample processing and protein quantification

The different batches of 2500 μL lyophilized hAMSCs secretome (Pools I-IV) and three samples of 2500 μL cell free lyophilized culture medium used as control samples (CTRL 1–3), were solubilized in 250 μL of water (LC-MS grade) to obtain 10× concentrated samples and gently vortexed to allow resolubilization. Bradford protein assay (Bio-Rad Laboratories, Hercules, CA, USA) was used to measure the total protein content of the samples by means of a UV–Vis spectrophotometer (8453 UV–Vis Supplies, Agilent Technologies, Waldbronn, Germany) using Bovine Serum Albumin (BSA) protein as reference.

2.3. Proteomic analysis

2.3.1. Chemicals

Iodoacetamide (IAA), D,L-dithiothreitol (DTT), ammonium bicarbonate (AMBIC), urea, Tris (hydroxymethyl) aminomethane and bovine serum albumin were from Sigma-Aldrich (St. Louis, MO, USA). Water, acetonitrile (ACN) and FASP centrifugal filter units Microcon 10, were from Merck (Darmstadt, Germany). All organic solvents were of LC-MS grade. Trypsin enzyme (Gold MS Grade) was from Promega (Madison, WI, USA). Formic acid (FA) (≥99 %, for LC-MS) was from VWR Chemicals (VWR International s.r.l., Milan, Italy). Protease inhibitor cocktail (PIC) was from Sigma-Aldrich (St. Louis, MO, USA).

2.3.2. Combined-FASP (C-FASP) sample pretreatment for proteomic analysis

C-FASP was performed by using centrifugal Microcon filter devices of 10 kDa molecular mass cut-off. With respect to the FASP protocol previously applied for hAMSCs secretome proteomic analysis [9] in C-FASP we introduced few modifications in order to collect the unretained filtrate free of urea for direct LC-MS analysis and characterization. Specifically, a secretome volume corresponding to a total protein content of 50 μg for each secretome pool was mixed with 0.1 % FA water solution (*v*/v), rather than urea buffer [9] up to reach the 200 μL loading volume, transferred to the filter device and centrifuged at 14000 ×*g* for 15 min. The replacement of urea buffer loading solution with 0.1 % FA water solution allowed to collect the C-FASP filtrate for direct proteomic analysis of small proteins and peptides, avoiding further steps of precipitation and purification. The filtrate, representing the <10 kDa proteome fraction, was compatible for intact form analysis, following a top-down approach, after the addition of the protease inhibitor (PIC) 1:20 (*v*/v, of 20× concentrated solution). The C-FASP supernatant, representing the proteome fraction >10 kDa retained by the filter, underwent instead to enzymatic digestion by bottom-up approach, following the procedure previously applied [9] after repeated cycles of filter washing with urea buffer to ensure efficient filter reconditioning from FA loading solution to proceed with trypsin protein digestion after disulfide bonds reduction and alkylation.

Both the proteome fractions resulting from C-FASP protocol were lyophilized and redissolved in 50 μL volume of 0.1 % FA solution before

LC-MS analysis, thus making their quali- and quantitative proteomic data fully comparable. Furthermore, the two fractions, since they are characterized by a similar molecular mass range, make use of the same LC-MS operating conditions for their analysis both for the characterization of the tryptic digested peptides in the fraction retained with C-FASP and for the small proteins and peptides in their intact form in the C-FASP filtrate, advantageously avoiding long time procedures of column change and reconditioning procedures and saving the total analysis time. Fig. 1 summarizes the workflow applied following application of C-FASP protocol to hAMSCs secretome proteomic analysis.

2.3.3. LC-MS analysis

LC-MS analyses were performed for each hAMSCs secretome pool in triplicate runs on UltiMate 3000 RSLCnano System coupled to Orbitrap Elite MS detector with EASY-Spray nanoESI source (Thermo Fisher Scientific, Waltham, MA, USA). The instrumental operation and data acquisition were carried out with the Thermo Xcalibur 2.2 computer program (Thermo Fisher Scientific). Chromatographic separations were performed on PepMap C18 EASY-Spray column (2 μm particles, 100 Å pore size) 15 cm in length x 50 μm of internal diameter (i.d.) (Thermo Fisher Scientific). The column was coupled to an Acclaim PepMap100 nano-trap cartridge (C18, 5 μm, 100 Å, 300 μm i.d. x 5 mm) (Thermo Fisher Scientific). Separation were performed at 40 °C in gradient elution using 0.1 % FA water solution as eluent A and ACN/FA solution (99.9:0.1, *v*/v) as eluent B as follows: (i) 5 % B (7 min), (ii) from 5 % to 35 % B (113 min), (iii) from 35 % B to 99 % (2 min), (iv) 99 % B (3 min), (v) from 99 % to 1.6 % B (2 min), (vi) 1.6 % B (3 min), (vii) from 1.6 % to 78 % B (3 min), (viii) 78 % B (3 min), (ix) from 78 % to 1.6 % B (3 min), (x) 1.6 % B (3 min), (xi) from 1.6 % to 78 % B (3 min), (xii) 78 % B (3 min), (xiii) from 78 % B to 5 % B (2 min), (xiv) 5 % B (20 min). The mobile phase flow rate was 0.3 μL/min. The injection volume was 5 μL. The Orbitrap Elite instrument operated in positive mode of ionization at full scan resolution of 60,000 in 350–2000 *m/z* acquisition range, performing MS/MS fragmentation by collision-induced dissociation (CID, 35 % normalized collision energy) of the 20 most intense signals of each MS spectrum in Data-Dependent Scan (DDS) mode. The minimum signal was set to 500.0, the isolation width to 2 *m/z* and the default charge state to +2. MS/MS spectra acquisition was performed in the linear ion trap at normal scan rate. MS/MS spectra acquisition in top-down analysis was at resolution of 60,000 and isolation width to 5 m/z.

2.3.4. Data analysis

LC-MS data were elaborated by the Xcalibur apparatus management software (Xcalibur 2.0.7 SP1, Thermo Fisher Scientific), and the Proteome Discoverer 1.4 software (version 1.4.1.14, Thermo Fisher Scientific) for protein characterization based on SEQUEST HT cluster as search engine against the Swiss-Prot *Homo Sapiens* proteome (UniProt knowledgebase Reviewed-Swiss-Prot, organism *Homo sapiens*, released in February 2022), and organism *Bos Taurus* (UniProt knowledgebase Reviewed-Swiss-Prot, organism *Bos Taurus*, released in April 2021) to identify proteins/peptides that may be present in the culture medium. The signal to noise ratio (S/N) threshold was set to 1.5. The set enzyme was trypsin with a maximum of 2 missed cleavage sites for LC-MS data elaboration obtained by bottom-up approach, while “no enzyme” was set for top-down analyses; minimum and maximum peptide length was 6 and 144 residues, respectively. Mass tolerance was 10 ppm; fragment mass tolerance was 0.5 Da and 0.02 Da; use average precursor mass False. Methionine oxidation (+15.99 Da) and acetylation N-Terminus (+42.011 Da) were set as dynamic modifications. For bottom-up analysis the carbamidomethylation of cysteine (+57.02 Da) was additionally set as static modification. Protein and peptide identification was validated by means of a decoy database search and calculation of the False Discovery Rate (FDR) statistical value by the Percolator node in Proteome Discoverer workflow by setting the FDR strict and relaxed target values at 0.01 and 0.05, respectively. Bottom-up identification results were filtered setting high confidence level of identification of at least 2 rank 1 peptides per protein with a minimum length of 9 amino acid residues, according to the HPP Mass Spectrometry Data Interpretation Guidelines [13]. The data obtained from the analysis of the <10 kDa fraction in the intact form were filtered by setting high confidence level of identification and peptide rank 1. Gene ontology (GO) analysis and classification was performed by PANTHER tool [18], using Fisher's Exact test type with false discovery rate (FDR) correction, the Reactome tool [19], and The Human protein Atlas database [20,21]. Functional protein interaction networks were analyzed by means of STRING tool [22] and Cytoscape (version 3.10.2) [23]. Grouping analysis was performed by Venn diagram tool (https://bioinfogp.cnb.csic.es/tools/venny/index.html) [24].

3. Results

3.1. Characterization of the hAMSCs secretome proteome fraction < 10 kDa

The proteome fraction unretained by the C-FASP filter was analyzed in its intact form. The molecular mass range of this fraction, below 10 kDa, was in fact suitable for application of a top-down proteomic approach investigating small proteins and peptides without previous enzymatic digestion. This approach is particularly interesting for characterizing isoforms and proteoforms of small proteins and peptides and

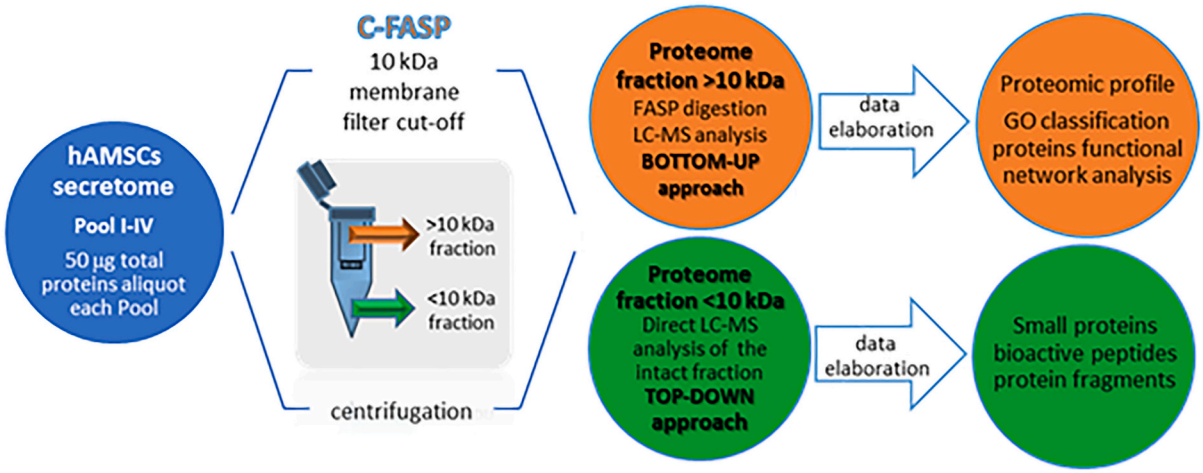

Fig. 1. Workflow of proteomic analysis and data elaboration by applying the C-FASP protocol.

to study and localize their post-translational modifications (PTMs).

The proteomic analysis of this fraction primarily focused on characterizing the peptidome of the hAMSC secretome, although the identification of small proteins below 10 kDa cannot be excluded. The study of the peptidome is an intriguing area of research, although it is generally proteomics that often serves as the initial step in the exploration of new biological matrices and materials. Beyond identifying endogenous peptides with relevant biological functions, peptidomic analysis includes the characterization of peptide fragments, referred to as the protein "fragmentome," which are generated by the intra- or extracellular proteins degradation occurring in vivo. This process is strongly influenced by different physiological and pathological conditions and aids in understanding specific protease activities and molecular processes associated with various states. Additionally, this includes the fascinating class of cryptides [25], which are peptide fragments with unique biological activities distinct from those of their parent proteins. Another important objective of peptidomic analysis is the characterization of peptides derived from non-coding RNAs, which are under investigation for their functions, roles in disease, and therapeutic potential [26,27].

The LC-MS analysis of the proteome fraction below 10 kDa of the hAMSC secretome, after data filtering for high confidence following the HPP Mass Spectrometry Data Interpretation Guidelines [13], identified 43, 22, 38 and 114 protein uniprot accessions in Pool I-IV, respectively. Each accession corresponding to a variable number of naturally occurring peptide fragments identified, 90, 39, 58 and 254, respectively (see Table S1 for identification data). Grouping analysis revealed a common set of 162 unique Uniprot accessions totally identified across all Pools with varying distributions across Pools I-IV (see Fig. 2), and represented by a variable number of naturally occurring peptide fragments. Particularly noteworthy is the consistent identification in all secretome Pools of six Uniprot accessions, namely Thymosin beta-4 and beta-10, Glyceraldehyde-3-phosphate dehydrogenase, alpha-Enolase, Collagen alpha-1(III), and alpha-1(I) chains (refer to Table 1). Importantly, these proteins and peptides were identified not in their full sequence, suggesting that they underwent proteolytic events pre- or post-secretion.

As shown in Table 1, the analysis identified different fragments of Thymosin beta-4 (TMSB4X) and beta-10 (TMSB10) peptides, two members of the Thymosins' family with an intact molecular mass around 5 kDa and characterized by non-conventional secretion, since lacking a signal peptide. Given their dual intracellular and extracellular location, their identification in the hAMSCs secretome is consistent and it

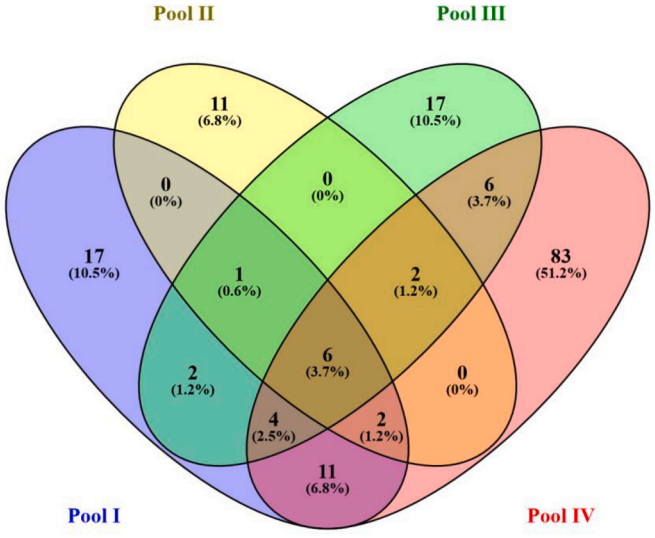

Fig. 2. Venn diagram grouping analysis of the proteins Uniprot accessions identified in Pools I-IV of the hAMSCs secretome by C-FASP by top-down approach.

potentially aligns with their known roles in cytoskeletal organization, cell motility, and biological functions encompassing wound healing, inflammation, tissue repair, and regeneration [28–31]. It is worthy of mention that specific sequence traits of Thymosin beta-4 peptide, such as AcSDKP and AcSDKPDMAEIEKFDKS (fragments 2–5 and 2–16, respectively, both N-terminal acetylated), are associated with anti-inflammatory and antiapoptotic properties, as well as the LKKTETQ sequence is linked to cell migration, wound healing, and pro-angiogenic activities [29]. The fact that Thymosin beta-4 undergoes successive hydrolyses steps by the action of meprin-α and prolyl oligopeptidase before generating the anti-inflammatory N-terminal peptide AcSDKP [32], could explain the extensive fragmentation frequently observed in biological matrices for this peptide. The peptide fragments of Thymosin beta-4 identified in the hAMSCs secretome interestingly include, partially or totally, these bioactive sequence traits. Of note, several of these peptide fragments have been already identified in other biological samples [33], therefore they could exhibit potential biological functions that should be further investigated.

Always in Table 1 we report the identification of several peptide fragments of Collagen alpha-1(I) chain (CO1A1), Collagen alpha-1(III) chain (CO3A1) and alpha-Enolase (ENOA), that are among the most abundant proteins identified by bottom-up approach in the retained fraction FASP [9] and C-FASP (see following paragraph 3.2). CO1A1 and CO3A1 are known substrates of metalloproteinases (MMPs) [34,35], therefore their extensive fragmentation observed in the <10 kDa hAMSCs secretome fraction could align with the prior identification of MMP1, MMP2, and MMP10 in the same secretome through the bottom-up approach [9]. Interestingly, the literature reported that recombinant Thymosin beta-4 has been found to regulate the expression of MMP-2 and metalloproteinase inhibitor 2 (TIMP-2) to promote tissue repair [36] and that the MMPs catalytic activity is necessary for Thymosin beta-4 to promote epithelial cell migration [37]. Speculatively, it could be hypothesized an interactive network involving beta-Thymosin peptides and Collagens, including MMPs, considering their roles in tissue repair and their MMPs regulation [34–37].

Interestingly alpha-Enolase (ENO1) and Glyceraldehyde-3-phosphate dehydrogenase (GAPDH), identified in this hAMSCs secretome fraction through their fragment peptides, have functional interactions as resulting by STRING network analysis and, moreover relevant, are substrates of MMP2, thus the previously hypothesized interactive network can be enlarged also to them (Fig. 3). TMSB4X and TMSB10 results a separate cluster of the network, although the previously described connection to MMP2 proteolytic activity [36,37]. Particularly, the Glyceraldehyde-3-phosphate dehydrogenase peptide fragments 201–215 and 324–335 are reported in Merops database [38] as generated by MMP2 enzyme proteolysis.

Recent studies [39,40] have identified new roles for both ENO1 and GAPDH in immunogenicity and immunomodulation, which align with their presence in the hAMSC secretome, known for its immunomodulatory properties. Specifically, alpha-enolase (ENO1) has been identified as a potential immunogenic molecule in human adipose tissue-derived mesenchymal stromal cells during allotransplantation [39]. Meanwhile, exogenous administration of GAPDH has been reported to modulate macrophage function by significantly reducing tumor necrosis factor (TNF)-α levels and inducing interleukin (IL)-10 production in response to LPS challenge. This suggests that extracellular GAPDH may promote the differentiation of macrophages into an intermediate M1/M2 phenotype, contributing to the resolution of inflammation [40].

3.2. Characterization of the hAMSCs secretome proteome fraction >10 kDa

The proteome fraction of the hAMSC secretome >10 kDa, which was retained by the FASP filter, underwent protein digestion with trypsin enzyme to enable in-depth proteomic exploration using a bottom-up approach. The LC-MS analysis conducted in triplicate for each sample

Table 1
List of the protein Uniprot accessions and relative fragment peptides repeatedly identified in the <10 kDa proteome fractions of the hAMSCs secretome Pools I-IV analyzed in intact form by LC-MS analysis.

Uniprot Accession Protein name	Fragment	Sequence	Modifications	MH+ [Da]
P62328	2–15	SDKPDMAEIEKFDK	N-Term(Acetyl)	1694.810
Thymosin beta-4	20–39	KTETQEKNPLPSKETIEQEK		2357.241
	20–44	KTETQEKNPLPSKETIEQEKQAGES		2829.421
	2–17	SDKPDMAEIEKFDKSK	N-Term(Acetyl)	1909.939
	33–44	ETIEQEKQAGES		1348.631
	21–44	TETQEKNPLPSKETIEQEKQAGES		2701.327
	21–32	TETQEKNPLPSK		1371.709
	21–39	TETQEKNPLPSKETIEQEK		2229.116
	26–44	NPLPSKETIEQEKQAGES		1984.977
P63313	2–17	ADKPDMGEIASFDKAK	N-Term(Acetyl)	1764.864
Thymosin beta-10	27–40	NTLPTKETIEQEKR		1686.897
	2–17	ADKPDMGEIASFDKAK	N-Term(Acetyl); M_6(Oxidation)	1780.859
	2–9	ADKPDMGE	N-Term(Acetyl)	904.375
	27–39	NTLPTKETIEQEK		1530.796
P06733	316-326	VGDDLTVTNPK		1158.603
alpha-Enolase	315–326	VVGDDLTVTNPK		1257.680
	258–269	DLDFKSPDDPSR		1391.648
	200–221	YGKDATNVGDEGGFAPNILENK		2309.103
	65–80	AVEHINKTIAPALVSK		1690.981
	81–92	KLNVTEQEKIDK		1444.795
	203–221	DATNVGDEGGFAPNILENK		1960.921
	203–228	DATNVGDEGGFAPNILENKEGLELLK		2743.377
	254–269	SGKYDLDFKSPDDPSR		1826.850
P02452	613–631	DGEAGAQGPPGPAGPAGER		1690.776
Collagen alpha-1(I)	1142–1154	GPPGSAGAPGKDG		1067.520
Chain	613–624	DGEAGAQGPPGP		1052.466
	539–552	GLTGSPGSPGPDGK		1226.600
	848–862	GPPGPIGNVGAPGAK		1288.712
	1043–1062	GPPGAPGAPGAPGPVGPAGK		1608.864
	287–304	GEPGSPGENGAPGQMGPR		1694.770
	560–572	GQDGRPGPPGPPG		1188.586
	1042–1062	AGPPGAPGAPGAPGPVGPAGK		1679.896
	893–903	GPPGPPGPAGK		931.506
	686–697	GVQGPPGPAGPR		1089.588
	649–672	AGPPGEAGKPGEQGVPGDLGAPGP		2112.056
	1118–1131	GPPGPPGSPGEQGP		1230.587
	557–568	GPAGQDGRPGPP		1105.538
	605–622	GAVGPAGKDGEAGAQGPP		1535.748
	599–622	GVPGPPGAVGPAGKDGEAGAQGPP		2040.026
	911–925	GETGPAGRPGEVGPP		1377.681
	1178–1190	GPPGPPGPPGPPG		1080.551
	1178–1196	GPPGPPGPPGPPGPPSAGF		1636.815
	1015–1026	EGAPGAEGSPGR		1084.503
	145–154	GPPGPPGPPG		829.427
	1181–1190			
P02461	597–610	GGPGGPGPQGPPGK		1159.584
Collagen alpha-1(III)	546–568	GSDGKPGPPGSQGESGRPGPPGP		2071.984
chain	537–568	GMPGSPGGPGSDGKPGPPGSQGESGRPGPPGP		2809.323
	1013–1024	DGNPGSDGLPGR		1141.524
	1025–1054	DGSPGGKGDRGENGSPGAPGAPGHPGPPGP		2633.231
	841–854	VAGPPGGSGPAGPP		1117.573
	945–956	GPLGIAGITGAR		1082.635
	543–568	GGPGSDGKPGPPGSQGESGRPGPPGP		2283.082
	183–194	GPPGTSGHPGSP		1047.484
	552–568	GPPGSQGESGRPGPPGP		1530.733
	552–566	GPPGSQGESGRPGPP		1376.659
	837–854	GPPGVAGPPGGSGPAGPP		1425.717
	606–620	GPPGKNGETGPQGPP		1389.674
	369–383	GEPGPQGHAGAQGPP		1356.631
	1173–1195	GSEGSPGHPGQPGPPGPPGPPGAPGP		1987.932
	623–637	TGPGGDKGDTGPPGP		1309.606
	537–568	GMPGSPGGPGSDGKPGPPGSQGESGRPGPPGP	M_2(Oxidation)	2825.302
	558–568	GESGRPGPPGP		1007.492
	467–485	DGSPGEPGANGLPGAAGER		1708.784
	1035–1054	GENGSPGAPGAPGHPGPPGP		1706.795
	537–562	GMPGSPG GPGSDGKPGPPGSQGESGR		2307.052
	1035–1060	GENGSPGAPGAPGHPGPPGPVGPAGK		2216.092
	1151–1166	DGTSGHPGPIGPPGPR		1498.736
	177–186	GPPGPPGPPG		829.427
P04406	281–294	VVSSDFNSDTHSST		1482.648
Glyceraldehyde-3- phosphate dehydrogenase	198–215	DGRGALQNIIPASTGAAK		1739.935
	201–215	GALQNIIPASTGAAK		1411.787
	324–335	VVDLMAHMASKE		1330.647

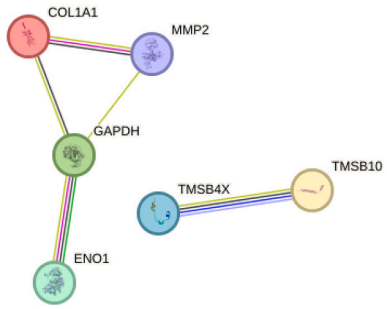

Fig. 3. Protein-protein functional network of the proteins identified through their fragment peptides in the proteome fraction <10 kDa of the hAMSCs secretome by LC-MS intact form analysis.

identified a total of 1043, 1212, 890, 1092 proteins in Pools I-IV, respectively. Adhering to stringent criteria of the HPP Data Interpretation Guidelines [13], we achieved high-confidence protein identifications, albeit resulting in a more concise yet reliable list. On average, proteomic analysis therefore identified 353 ± 44 proteins across Pools I-IV (see Table S2). A comprehensive grouping analysis revealed a total of 597 unique protein elements totally identified and differentially distributed among the Pools. A group of 163 proteins have been consistently identified across all pools (Fig. 4, left panel). Comparative analysis between the results obtained using the C-FASP approach and those from the previously applied FASP method [9] showed substantial overlap (Fig. 4, right panel), reflecting robust similarity in the identification capabilities of the two protocols. The observed 12–15 % variance is consistent with the biological variability inherent in biomaterials. Notably, 137 proteins were identified by both methods (listed in Table S3), collectively defining the repeatable core protein profile of the hAMSCs secretome.

Considering the protein area values obtained by label-free relative quantitation, resulting from Proteome Discoverer elaboration of the LC-MS raw data (data in supplementary Table S2), the following proteins resulted the most abundant in the hAMSCs secretome (considering protein area values $>5 \times 10^7$), namely, albumin (ALBU), collagen alpha-1(I) chain (CO1A1), metalloproteinase inhibitor 1 (TIMP1), fibronectin (FINC), collagen alpha-1(III) chain (CO3A1), calmodulin-3 (CALM3), L-lactate dehydrogenase A (LDHA), triosephosphate isomerase (TPIS), SPARC (SPRC), calreticulin (CALR), peptidyl-prolyl cis-trans isomerase B (PPIB), cathepsin B (CATB), peroxiredoxin-1 (PRDX1), galectin-1 (LEG1), alpha-enolase (ENO1), transgelin (TAGL), follistatin-related protein 1 (FSTL1) and protein disulfide-isomerase A3 (PDIA3).

3.2.1. Gene ontology and protein-protein functional interaction analysis

The group of 137 common proteins robustly identified in hAMSCs secretome by bottom-up approach was explored for protein-protein functional interactions and pathway overrepresentation analysis by STRING tool (high confidence analysis 0.7) and exported to Cytoscape. The resulting network showed only few disconnected nodes (Fig. 5), evidencing strong functional interactions between the analyzed proteins. Yellow nodes represent the extracellular proteins in the network, which are predominant. Additional node colors highlight various functional categories and localizations, including extracellular space, extracellular region, extracellular vesicle, extracellular membrane-bounded organelle, and extracellular organelle. Table S4 shows the results of the functional enrichment analysis of the network nodes. Different protein domains were significantly enriched in the network, including the Intermediate filament protein, Calponin homology domain, Thrombospondin N-terminal-like domains, Filamin-type immunoglobulin domains, Fibrillar collagens C-terminal domain, Epidermal growth factor-like domain and Tissue inhibitor of metalloproteinase family, already described in our previous investigation [9].

It is noteworthy that many of these domains characterize cytoskeletal proteins and have a role in cytoskeletal signaling and dynamics, and in extracellular matrix [41,42]. One hundred and twenty-two Reactome pathways resulted significantly enriched in the network and, interestingly, the Immune System, Metabolism of proteins, Signal Transduction, Innate Immune System, Extracellular matrix organization and Hemostasis, showing the highest protein counts.

Considering instead the 163 proteins totally identified by C-FASP and bottom-up approach, the enrichment analysis by Reactome tool confirmed the pathways of Immune System, Hemostasis, and Extracellular Matrix Organization pathways, mostly related to the biological activities of the hAMSCs secretome, as included in the top 25 over-represented, also showing the highest number of protein counts (Table S5).

Interestingly, the Gene Ontology (GO) over-representation analysis of the Biological process by PANTHER tool showed the negative regulation of angiogenesis (GO:0016525), glycolytic process (GO:0006096), regulation of response to wounding (GO:1903034), regulation of wound healing (GO:0061041), cellular response to reactive oxygen species (GO:0034614), hexose biosynthetic process (GO:0019319), regulation of angiogenesis (GO:0045765) and the regulation of vasculature development (GO:1901342), as significantly enriched (Fig. 6). The over-representation analysis of the Molecular functions (Fig. 7) showed the fold enrichment of the protein disulfide isomerase activity (GO:0003756), collagen binding (GO:0005518), protease binding (GO:0002020), extracellular matrix binding (GO:0050840), protein-disulfide reductase activity (GO:0015035), disulfide oxidoreductase activity (GO:0015036), metalloaminopeptidase activity (GO:0070006),

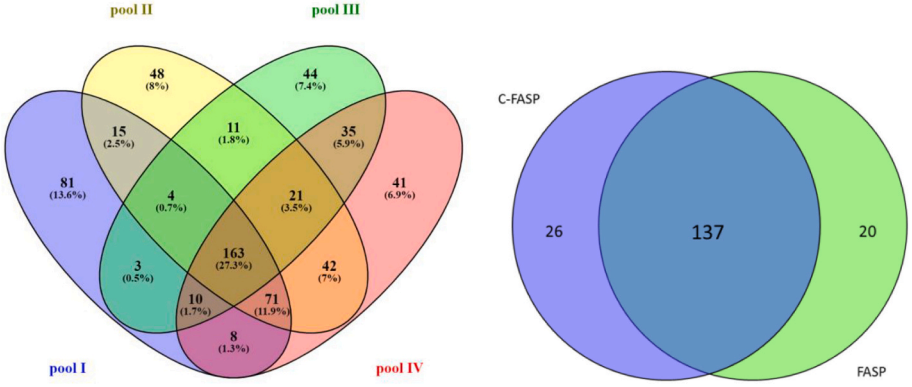

Fig. 4. Venn diagram grouping analysis of the proteins identified by bottom-up approach in the >10 kDa proteome fraction of the hAMSCs secretome Pools I-IV obtained after the modified C-FASP protocol applied in the present study (left panel). In the right panel the list of the secretome Pools l I-IV common proteins (i.e. 163 elements) have been compared by grouping analysis with the common proteins identified in our previous investigation by FASP (i.e. 157 elements) [11].

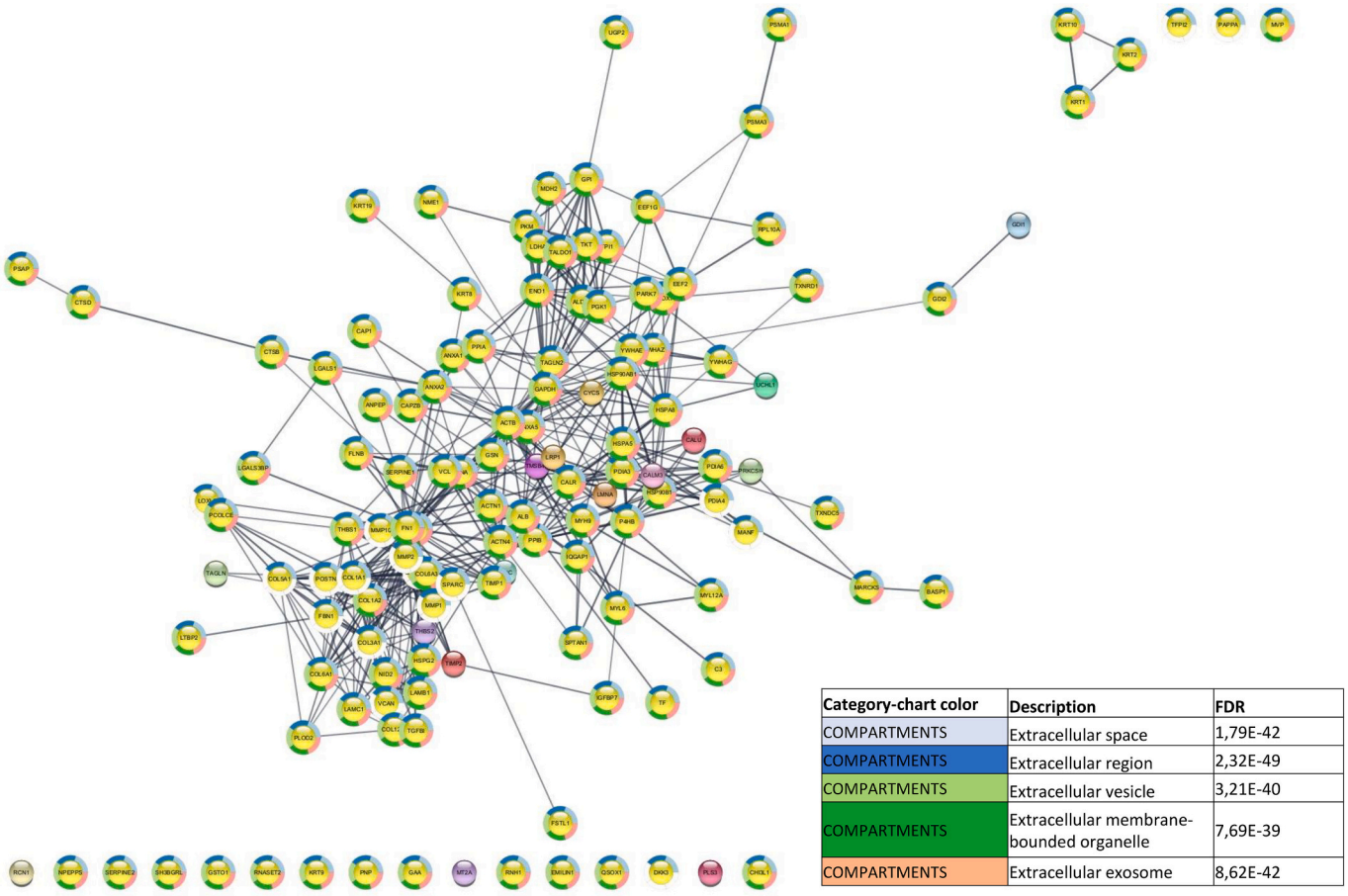

Fig. 5. Visualization of a protein interaction network generated with STRING and Cytoscape (version 3.10.2) in high confidence 0.7. Nodes represent the 137 hAMSCs secretome core proteins identified by bottom-up approach, while edges indicate physical interactions between them. Node colors denote functional categories and localization: light blue "extracellular space," blue "extracellular region," light green "extracellular vesicle," dark green "extracellular membrane-bounded organelle," pink for "extracellular organelle." Yellow nodes indicate extracellular proteins. In the lower part of the figure, disconnected nodes are shown separately. (For interpretation of the references to colour in this figure legend, the reader is referred to the web version of this article.)

aminopeptidase activity (GO:0004177), oxidoreductase activity, acting on a sulfur group of donors (GO:0016667), extracellular matrix structural constituent (GO:0005201), isomerase activity (GO:0016853), antioxidant activity (GO:0016209) and actin filament binding (GO:0051015), consistent with the biological properties of the hAMSCs secretome.

3.3. C-FASP analysis of control samples

To eliminate the influence of components of the medium on the characterization of the hAMSCs secretome, three distinct control samples consisting of DMEM-F12 media (CTRL 1–3) were analyzed by C-FASP, and the results compared with the hAMSCs secretome following LC-MS data elaboration against both the *Homo sapiens* and *Bos taurus* databases. Concerning the bottom-up data of the >10 kDa proteome fraction, the proteins consistently identified in all CTRL samples included only Albumin and various Keratins, aligning with prior observations from FASP analysis [9]. These identifications were attributed to potential contaminations commonly encountered in proteomic analyses. In the context of top-down identification data, the grouping analysis conducted on CTRL samples 1–3 revealed no proteins shared with those identified in the secretome pools (data in supplementary File S1). This outcome excluded contributions from the medium components to protein identification in the hAMSCs secretome.

4. Discussion

The secretome of human amniotic mesenchymal stromal cells (hAMSCs) is emerging as a promising alternative to cell therapy in tissue regeneration, owing to its potent immunomodulatory and pro-regenerative effects [1]. While proteomic analyses of hAMSC and other MSC secretomes have been extensively studied [9,43,44], this study introduces a modified method for analyzing the hAMSC secretome with a focus on both high- and low-molecular-mass fractions of the same sample aliquot analyzed. The hAMSCs secretome possesses immunomodulatory capabilities involving molecules both below 3 kDa and above 100 kDa [12]. Proteomic analysis of the molecular mass fraction above 100 kDa employs a bottom-up approach, where enzymatic digestion precedes mass spectrometry characterization. In contrast, the molecular mass fraction below 3 kDa can be directly examined intact using a top-down approach, although this strategy is mostly referred to the analysis of intact small proteins. In our previous study [9], we used FASP with a 10 kDa molecular cut-off to profile the hAMSCs secretome proteome. However, this method discarded the fraction not retained by the molecular mass filter membrane, focusing only on the proteome fraction above the 10 kDa cut-off. This led to the possible omission of crucial information on small proteins and peptides, including the <3 kDa fraction essential for immunomodulatory activity [12]. To address this limitation, we applied a Filter Aided Sample Preparation (FASP) protocol with few modifications, that we named Combined-FASP (C-FASP), in order to combine different proteomic approaches to the FASP

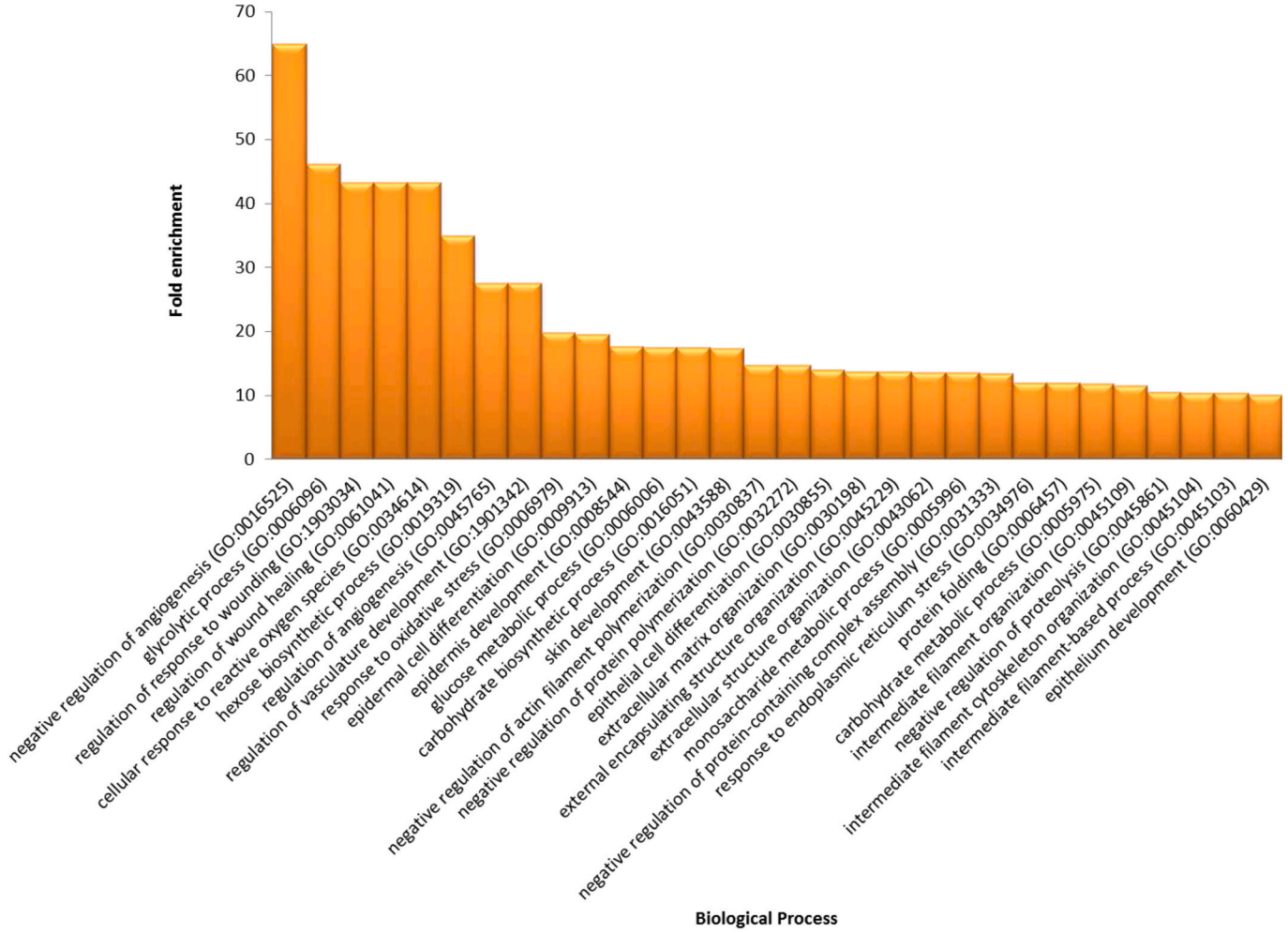

Fig. 6. Biological processes resulted significantly enriched by PANTHER tool analysis of the 137 proteins repeatedly identified in the hAMSCs secretome following the bottom-up approach. Results were filtered for a fold enrichment value ≥10.

filter retained and the unretained proteome fractions following same sample preparation in one-step and to complement their data, fully comparable from quali- and quantitative point of view, for a comprehensive characterization covering low and high molecular mass range.

To facilitate LC-MS analysis of the smaller proteome fraction not retained by the filter, the C-FASP protocol replaces the urea loading buffer [9] with a 0.1 % formic acid water solution (*v*/v). This modification allows the collection of the filtrate (i.e., the fraction <10 kDa) resulting from first centrifugation of the loaded sample, enabling its direct LC-MS analysis. Simultaneously, the protein fraction retained by the filter (>10 kDa) undergoes the FASP digestion protocol, following the same procedure as described previously [9]. Furthermore, an increased number of urea buffer washing steps after sample loading are implemented to ensure efficient buffer exchange and filter preconditioning for subsequent steps of protein reduction, alkylation, and enzymatic digestion.

By processing the same sample aliquot, we generated a low molecular fraction of intact small proteins and peptides and a high molecular fraction of enzymatically digested proteins, resulting in proteolytic peptides. Both fractions can be analyzed using the same LC-MS instrumentation and operating conditions. Therefore, in addition to saving sample quantity, C-FASP significantly reduces the total analysis time for a comprehensive proteomic investigation. However, it's important to note that the use of the C-FASP approach is limited to protein samples that do not contain surfactants or urea, as these compounds do not end up in the filtrate after the initial centrifugation. This limitation makes C-FASP particularly advantageous for proteomic analysis of conditioned media, such as the hAMSCs secretome, which was the focus of the present investigation.

Our analysis of the four secretome pools using a bottom-up approach identified an average of 1059 ± 133 proteins. However, this number was significantly reduced after applying the stringent criteria recommended by the Human Proteome Project Data Interpretation Guidelines of HUPO [13], ensuring high-confidence identifications. As a result, a total of 597 unique proteins were identified across the four analyzed pools, with varying distributions. The number of identified proteins ranged from 291 in Pool III to 391 in Pool IV (see Table S2 for details).

Regarding the number of total proteins identified, our results are aligned with those from other proteomic studies on MSC-derived secretomes from various sources [44–46]. These findings underscore the influence of cell type, culture conditions, and experimental factors on secretome protein composition.

Furthermore, we observed donor-associated variability in the proteomic profiles of MSC secretomes. While this issue has been addressed in several other studies [44–46], only one study has reported the specific individual data documenting the proteomic differences in individual BM-MSC secretomes related to different donors [43]. These individual differences likely reflect the inherent heterogeneity of MSC populations, which include progenitor cells, committed progenitors, and differentiated cells in varying proportions across donors [47]. Factors such as donor age, gender, and medication use further contribute to this variability, affecting not only the MSCs themselves but also their secretomes.

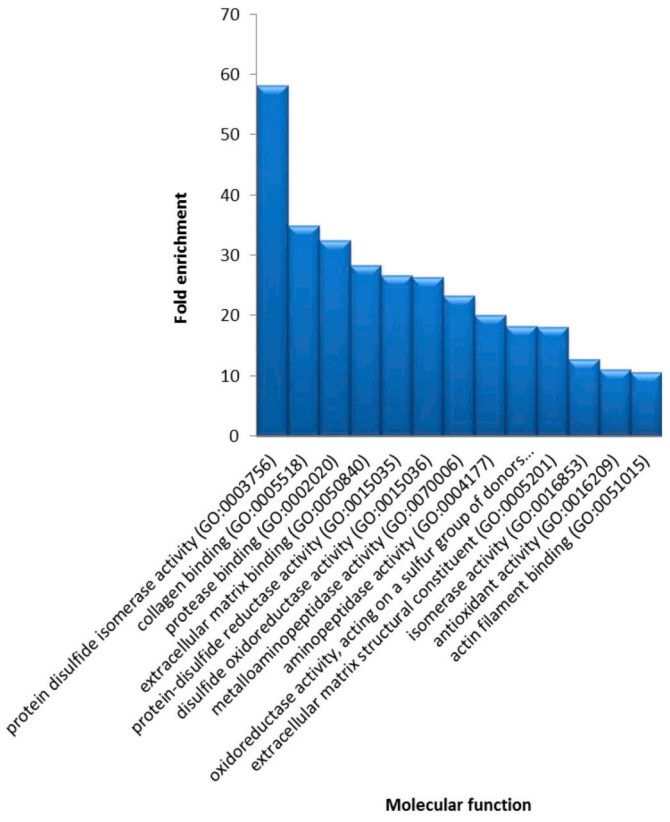

Fig. 7. Molecular functions resulted significantly enriched by PANTHER tool analysis of the 137 proteins repeatedly identified in the hAMSCs secretome following the bottom-up approach. Results were filtered for a fold enrichment value ≥10.

For example, recent single-cell RNA-seq studies have shown that MSC cytokine secretion varies based on tissue origin and donor characteristics [48].

However, despite the observed proteomic differences among hAMSC secretome pools, their immunomodulatory potential remained consistent (data not shown). We hypothesize that the key molecules driving this activity reside among the 163 proteins common to all tested pools, suggesting that pooling secretomes from multiple donors could mitigate variability and preserve therapeutic efficacy.

Furthermore, the analysis of the hAMSC secretome proteome fraction below 10 kDa allowed to first investigate the naturally occurring peptidome of the hAMSCs secretome, revealing specific peptide fragments of proteins and peptides involved in wound healing, anti-inflammatory response, tissue repair and regeneration processes, such as fragments of Thymosin beta-4 and beta-10, Glyceraldehyde-3-phosphate dehydrogenase, alpha-Enolase, and Collagen alpha-1(III) and alpha-1(I) chains, with biological significance to be deeply investigated in future studies. The consistent identification of these entities across different pools indicates their potential relevance in the biological activities mediated by the hAMSC secretome. Moreover, the detection of peptide fragments rather than intact sequences of these entities implies proteolytic events, highlighting the dynamic nature of the secretome. This dynamic nature underscores the importance of considering both full-length proteins and their fragments in understanding the functional properties of the hAMSC secretome. The identification of beta-Thymosins, known for diverse biological functions, underscores their potential role in the immunomodulatory and regenerative properties of the hAMSCs secretome. Specific sequence traits associated with anti-inflammatory, antiapoptotic, cell migration, wound healing, and pro-angiogenic activities provide a basis for further exploration of the functional significance of these peptide fragments identified, which could exert specific biological roles. Furthermore, the identification of collagen fragments, particularly those of Collagen alpha-1(I) and alpha-1(III) chains, along with alpha-Enolase and GAPDH, suggests a complex interplay within the secretome. The involvement of metalloproteinases (MMPs) in the proteolytic processing of collagen substrates aligns with the identification of MMPs in the bottom-up approach. The potential interactive network involving beta-Thymosins, collagens, alpha-Enolase, Glyceraldehyde-3-phosphate dehydrogenase and MMPs provides a plausible mechanism for the observed biological activities, linking tissue repair and immumodulation with potential regulation of MMPs expression. The identification of beta-Thymosin peptides and collagens, along with their extensive fragmentation observed, might result from MMPs activity in the hAMSCs secretome. Interestingly, MMPs' catalytic activity is reported to be necessary for thymosin beta-4 to promote epithelial cell migration [37].

The integration of proteomic data from both the retained and unretained fractions of the FASP filter membrane provides a comprehensive overview of the hAMSC secretome's protein phenotype, setting the stage for deeper exploration into the molecular mechanisms that drive its immunomodulatory, anti-inflammatory, and tissue regeneration capabilities, all of which hold significant promise for regenerative medicine. Our bottom-up proteomic analysis of the FASP-retained fraction identified 137 core proteins, reinforcing our earlier findings [9].

Protein-protein functional interaction mapping identified a network enriched with key protein domains, prominently featuring cytoskeletal proteins. This underscores the pivotal roles of cytoskeletal dynamics, signaling pathways, and extracellular matrix interactions in the hAMSC secretome's functionality. The proteins identified play significant roles in immune response, hemostasis, and extracellular matrix organization, highlighting their potential contributions to the secretome's therapeutic effects.

Notably, the identified proteins include intracellular components, an unexpected finding given the stringent filtration of the hAMSC secretome through 0.2 μm sterilizing filters, specifically designed to exclude cell debris. It has been suggested that apoptotic bodies and membrane fragments typically exceed 0.2 μm, making their presence in the filtered secretome improbable [49]. Nonetheless, intracellular proteins have been detected, likely encapsulated within extracellular vesicles (EVs), despite the removal of larger debris such as apoptotic bodies and microvesicles. For example, tumor-derived EVs have been shown to contain cytoskeletal proteins, including actin and tubulin, which are typically classified as intracellular and play critical roles in maintaining cellular structure and transport, as well as heatshock proteins (Hsp 70 and 90) and other type of proteins involved in extracellular matrix processes as well as markers of proliferation such as Mib1 and CTGF [50]. Others have identified proteins such as Syntenin and Aquaporin 1 in EV fractions, indicating that intracellular proteins involved in signaling and water transport can also be secreted through EVs [51]. Similarly, another group reported the presence of pathological proteins associated with amyotrophic lateral sclerosis (ALS) being transported by EVs, such as FUS or TDP43 that are prevalently localized in the nucleus or cytoplasm, highlighting their role in disseminating disease-associated intracellular proteins [52].

These findings are in line with our recent work, in which we characterized the proteomic profile of vesicular fractions isolated from the hAMSC secretome using Field-Flow Fractionation (FFF [53]. Interestingly, EVs isolated from the hAMSC secretome contained proteins such as SPARC, annexins, serpins, heat shock proteins and others that are typically considered intracellular molecules [53]. Our results suggest that intracellular proteins are most likely transported through EVs and exosomes, which serve as key mediators of intercellular communication, carrying diverse biomolecules such as mRNA, miRNA, and proteins crucial for cellular metabolism and structural organization. Our investigation not only catalogs the full spectrum of proteins present in the hAMSC secretome but also emphasizes the critical need to understand the entire proteome profile to elucidate protein interactions and their in

vivo activities. This study provides valuable insights into the unique properties of the hAMSC secretome, which, unlike those from other MSC sources, is distinguished by its diverse profile of proteins and peptides, including those under 3 kDa and over 100 kDa. This distinctive molecular composition is likely responsible for its enhanced regenerative and immunomodulatory effects [9,43,44].

Employing the Combined-FASP (C-FASP) protocol allowed for the simultaneous analysis of both retained and unretained secretome fractions, leading to the discovery of hAMSCs peptidome including interesting fragments of Thymosin beta-4 and beta-10 peptides, of collagen and of enzymes like alpha-Enolase and Glyceraldehyde-3-phosphate dehydrogenase, less commonly found in the secretomes of other MSCs and not been identified in other studies [43,45,46], suggesting that the hAMSC secretome may have enhanced immunomodulatory and regenerative properties. This potential is further supported by the presence of proteins and peptides crucial for immune modulation and tissue repair. Moreover, the dynamic nature of the hAMSC secretome, characterized by extensive proteolytic processing, underscores the necessity of considering both intact proteins and their fragments to fully understand its functional properties. This comprehensive characterization not only sheds light on the molecular mechanisms driving the therapeutic potential of hAMSCs but also paves the way for future research aimed at harnessing these unique properties for regenerative medicine applications.

5. Conclusions

The proteomic characterization of cell secretomes presents significant challenges due to the typically low concentrations of proteins and peptides involved [54]. Traditionally, using the Filter-Aided Sample Preparation (FASP) method for secretome analysis has been particularly demanding, as it necessitates purification, digestion, and concentration prior to liquid chromatography-mass spectrometry (LC-MS) analysis. In this study, we adapted the FASP protocol with slight modifications from our previous work to enable combined proteomic and peptidomic characterization from the same sample aliquot. This innovative approach, termed Combined-FASP (C-FASP), integrates different proteomic analytical approaches within a single streamlined processing step, facilitating a comprehensive characterization of the proteome and peptidome across a broad molecular mass range. This not only optimizes analysis time but also significantly reduces the sample volume requirements, an essential advantage when working with limited sample quantities.

Our study provides several novel contributions to the field. Firstly, we successfully identified by bottom-up approach a group of core proteins in the hAMSCs secretome which repeatedly characterize the FASP retained fraction. More importantly, we conducted a pioneering peptidomic analysis of the hAMSC secretome by examining the FASP unretained fraction below 10 kDa, an area previously unexplored except for a single metabolomic study [55]. This dual approach allows for the first-time identification of naturally occurring peptides and protein fragments which characterize the biological matrix, providing a more complete understanding of the secretome's composition.

These findings advance the current scientific literature by establishing a consistent and reproducible molecular profile that defines the hAMSC secretome and its biological activity. The identification of both protein and peptide components enhances our understanding of the molecular mechanisms underlying its potent immunomodulatory and anti-inflammatory actions. This enriched knowledge base is pivotal for developing innovative therapeutic strategies in regenerative medicine and offers new avenues for treating inflammatory-based diseases, highlighting the hAMSC secretome's potential as a distinctive and valuable resource in medical research and application.

Funding

This research was funded by PRIN 2017 program of Italian Ministry of Research and University (MIUR, Grant No. 2017RSAFK7), MIUR 5 × 1000, *Contributi per il finanziamento degli Enti privati che svolgono attività di ricerca - CEPR*, and intramural funds at Università Cattolica del Sacro Cuore (Linea D1).

CRediT authorship contribution statement

Alexandra Muntiu: Writing – review & editing, Writing – original draft, Visualization, Methodology, Investigation, Formal analysis, Data curation. **Andrea Papait:** Writing – review & editing, Visualization, Methodology, Investigation, Data curation. **Federica Vincenzoni:** Writing – review & editing, Visualization, Methodology, Investigation, Data curation. **Diana Valeria Rossetti:** Writing – review & editing, Visualization, Methodology, Investigation, Formal analysis, Data curation. **Pietro Romele:** Writing – review & editing, Visualization, Methodology, Investigation, Data curation. **Anna Cargnoni:** Writing – review & editing, Visualization, Methodology, Investigation, Data curation. **Antonietta Silini:** Writing – review & editing, Visualization, Methodology, Investigation, Data curation. **Ornella Parolini:** Writing – review & editing, Visualization, Supervision, Methodology, Investigation, Funding acquisition, Data curation, Conceptualization. **Claudia Desiderio:** Writing – review & editing, Writing – original draft, Visualization, Supervision, Methodology, Investigation, Funding acquisition, Formal analysis, Data curation, Conceptualization.

Declaration of competing interest

The authors declare that they have no known competing financial interests or personal relationships that could have appeared to influence the work reported in this paper. All authors have read and approved the manuscript final version.

Data availability

The mass spectrometry proteomic data have been deposited to the ProteomeXchange Consortium via the PRIDE [56] partner repository with the dataset identifier PXD055623.

Appendix A. Supplementary data

Supplementary data to this article can be found online at https://doi.org/10.1016/j.jprot.2024.105339.

References

[1] A.R. Silini, M. Magatti, A. Cargnoni, O. Parolini, Is immune modulation the mechanism underlying the beneficial effects of amniotic cells and their derivatives in regenerative medicine? Cell Transplant. 26 (2017) 531–539, https://doi.org/10.3727/096368916X69369.

[2] Y. Fu, J. Ji, F. Shan, J. Li, R. Hu, Human mesenchymal stem cell treatment of premature ovarian failure: new challenges and opportunities, Stem Cell Res Ther 12 (2021) 1–13, https://doi.org/10.1186/s13287-021-02212-0.

[3] N. Eiro, M. Fraile, A. González-Jubete, L.O. González, F.J. Vizoso, Mesenchymal (stem) stromal cells based as new therapeutic alternative in inflammatory bowel disease: basic mechanisms, experimental and clinical evidence, and challenges, Int. J. Mol. Sci. 23 (2022) 8905, https://doi.org/10.3390/ijms23168905.

[4] E. Ragni, A. Papait, C. Perucca Orfei, A.R. Silini, A. Colombini, M. Viganò, L. De Girolamo, Amniotic membrane-mesenchymal stromal cells secreted factors and extracellular vesicle-miRNAs: anti-inflammatory and regenerative features for musculoskeletal tissues, Stem Cells Transl. Med. 10 (2021) 1044–1062, https://doi.org/10.1002/sctm.20-0390.

[5] H. Skalnikova, J. Motlik, S.J. Gadher, H. Kovarova, Mapping of the secretome of primary isolates of mammalian cells, stem cells and derived cell lines, Proteomics 11 (2011) 691–708, https://doi.org/10.1002/pmic.201000402.

[6] D. He, F. Zhao, H. Jiang, Y. Kang, Y. Song, X. Lin, X. Pang, LOXL2 from human amniotic mesenchymal stem cells accelerates wound epithelialization by promoting differentiation and migration of keratinocytes, Aging (Albany NY) 12 (2020) 12960–12986, https://doi.org/10.18632/aging.103384.

[7] F.A. Dabrowski, A. Burdzinska, A. Kulesza, A. Sladowska, A. Zolocinska, K. Gala, M. Wielgos, Comparison of the paracrine activity of mesenchymal stem cells derived from human umbilical cord, amniotic membrane, and adipose tissue, J. Obstet. Gynaecol. Res. 43 (2017) 1758–1768, https://doi.org/10.1111/jog.13432.

[8] J.W. Hur, M.S. Kim, S.Y. Oh, H.Y. Kang, J. Bae, H. Kim, D.H. Park, Label-free quantitative proteome profiling of cerebrospinal fluid from a rat stroke model with stem cell therapy, Cell Transplant. 30 (2021), https://doi.org/10.1177/09636897211023474, 9636897211023474.

[9] A. Muntiu, A. Papait, F. Vincenzoni, A. Vitali, W. Lattanzi, P. Romele, A. Cargnoni, A. Silini, O. Parolini, C. Desiderio, Disclosing the molecular profile of the human amniotic mesenchymal stromal cell secretome by filter-aided sample preparation proteomic characterization, Stem Cell Res Ther 14 (2023) 339, https://doi.org/10.1186/s13287-023-03557-4.

[10] J.R. Wiśniewski, Filter-aided sample preparation for proteome analysis, Methods Mol. Biol. 2018 (1841) 3–10, https://doi.org/10.1007/978-1-4939-8695-8_1.

[11] J.R. Wiśniewski, Filter aided sample preparation - a tutorial, Anal. Chim. Acta 1090 (2019) 23–30, https://doi.org/10.1016/j.aca.2019.08.032.

[12] D. Rossi, S. Pianta, M. Magatti, P. Sedlmayr, O. Parolini, Characterization of the conditioned medium from amniotic membrane cells: prostaglandins as key effectors of its immunomodulatory activity, PLoS One 7 (2012) 46956, https://doi.org/10.1371/journal.pone.0046956.

[13] E.W. Deutsch, L. Lane, C.M. Overall, N. Bandeira, M.S. Baker, C. Pineau, R. L. Moritz, F. Corrales, S. Orchard, J.E. Van Eyk, Y.K. Paik, S.T. Weintraub, Y. Vandenbrouck, G.S. Omen, Human proteome project mass spectrometry data interpretation guidelines 3.0, J. Proteome Res. 18 (2019) 4108–4116, https://doi.org/10.1021/acs.jproteome.9b00542.

[14] M. Magatti, S. Pianta, A. Silini, O. Parolini, Isolation, culture, and phenotypic characterization of mesenchymal stromal cells from the amniotic membrane of the human term placenta, Methods Mol. Biol. 1416 (2016) 233–244, https://doi.org/10.1007/978-1-4939-3584-013.

[15] M. Dominici, K. Le Blanc, I. Mueller, I. Slaper-Cortenbach, F. Marini, D. Krause, R. Deans, A. Keating, D.J. Prockop, E. Horwitz, Minimal criteria for defining multipotent mesenchymal stromal cells. The International Society for Cellular Therapy position statement, Cytotherapy 8 (2006) 315–317, https://doi.org/10.1080/14653240600855905.

[16] O. Parolini, F. Alviano, G.P. Bagnara, G. Bilic, H.J. Bühring, M. Evangelista, S. Hennerbichler, B. Liu, M. Magatti, N. Mao, T. Miki, F. Marongiu, H. Nakajima, T. Nikaido, C.B. Portmann-Lanz, V. Sankar, M. Soncini, G. Stadler, D. Surbek, T. A. Takahashi, H. Redl, N. Sakuragawa, S. Wolbank, S. Zeisberger, A. Zisch, S. C. Strom, Concise review: isolation and characterization of cells from human term placenta: outcome of the first international workshop on placenta derived stem cells, Stem Cells 26 (2008) 300–311, https://doi.org/10.1634/stemcells.2007-0594.

[17] A.R. Silini, A. Papait, A. Cargnoni, E. Vertua, P. Romele, P. Bonassi Signoroni, M. Magatti, S. De Munari, A. Masserdotti, A. Pasotti, S. Rota Nodari, G. Pagani, M. Bignardi, O. Parolini, CM from intact hAM: an easily obtained product with relevant implications for translation in regenerative medicine, Stem Cell Res Ther 12 (2021) 540, https://doi.org/10.1186/s13287-021-02607-z.

[18] H. Mi, X. Huang, A. Muruganujan, H. Tang, C. Mills, D. Kang, P.D. Thomas, PANTHER version 11: expanded annotation data from gene ontology and Reactome pathways, and data analysis tool enhancements, Nucleic Acids Res. 45 (2017) D183–D189, https://doi.org/10.1093/nar/gkw1138.

[19] A. Fabregat, K. Sidiropoulos, G. Viteri, O. Forner-Martinez, P. Marin-Garcia, V. Arnau, P. D'Eustachio, L. Stein, H. Hermjakob, Reactome pathway analysis: a high-performance in-memory approach, BMC Bioinform. 18 (2017) 1–9, https://doi.org/10.1186/s12859-017-1559-2.

[20] M. Uhlen, P. Oksvold, L. Fagerberg, E. Lundberg, K. Jonasson, M. Forsberg, M. Zwahlen, C. Kampf, K. Wester, S. Hober, H. Wernerus, L. Björling, F. Ponten, Towards a knowledge-based human protein atlas, Nat. Biotechnol. 28 (2010) 1248–1250, https://doi.org/10.1038/nbt1210-1248.

[21] M. Uhlén, M.J. Karlsson, A. Hober, A.S. Svensson, J. Scheffel, D. Kotol, W. Zhong, A. Tebani, L. Strandberg, F. Edfors, E. Sjöstedt, J. Mulder, A. Mardinoglu, A. Berling, S. Ekblad, M. Dannemeyer, S. Kanje, J. Rockberg, M. Lundqvist, M. Malm, A.L. Volk, P. Nilsson, A. Månberg, T. Dodig-Crnkovic, E. Pin, M. Zwahlen, P. Oksvold, K. von Feilitzen, R.S. Häussler, M.G. Hong, C. Lindskog, F. Ponten, B. Katona, J. Vuu, E. Lindström, J. Nielsen, J. Robinson, B. Ayoglu, D. Mahdessian, D. Sullivan, P. Thul, F. Danielsson, C. Stadler, E. Lundberg, G. Bergström, A. Gummesson, B.G. Voldborg, H. Tegel, S. Hober, B. Forsström, J. M. Schwenk, L. Fagerberg, Å. Sivertsson, The human secretome, Sci. Signal. 12 (2019) eaaz0274, https://doi.org/10.1126/scisignal.aaz0274.

[22] D. Szklarczyk, A.L. Gable, D. Lyon, A. Junge, S. Wyder, J. Huerta-Cepas, M. Simonovic, N.T. Doncheva, J.H. Morris, P. Bork, L.J. Jensen, C.V. Mering, STRING v11: protein-protein association networks with increased coverage, supporting functional discovery in genome-wide experimental datasets, Nucleic Acids Res. 47 (2019) D607–D613, https://doi.org/10.1093/nar/gky1131.

[23] P. Shannon, A. Markiel, O. Ozier, N.S. Baliga, J.T. Wang, D. Ramage, N. Amin, B. Schwikowski, T. Ideker, Cytoscape: a software environment for integrated models of biomolecular interaction networks, Genome Res. 13 (2003) 2498–2504, https://doi.org/10.1101/gr.1239303.

[24] J.C. Oliveros, Venny. An interactive tool for comparing lists with Venn's diagrams, 2007-2015. https://bioinfogp.cnb.csic.es/tools/venny/index.html.

[25] F. Iavarone, C. Desiderio, A. Vitali, I. Messana, C. Martelli, M. Castagnola, T. Cabras, Cryptides: latent peptides everywhere, Crit. Rev. Biochem. Mol. Biol. 53 (2018) 246–263, https://doi.org/10.1080/10409238.2018.1447543.

[26] S. Wang, C. Mao, S. Liu, Peptides encoded by noncoding genes: challenges and perspectives, Sig. Transduct. Target Ther. 4 (2019) 57, https://doi.org/10.1038/s41392-019-0092-3.

[27] S.Z. Bakhti, S. Latifi-Navid, Non-coding RNA-encoded peptides/proteins in human Cancer: the future for Cancer therapy, Curr. Med. Chem. 29 (22) (2022) 3819–3835, https://doi.org/10.2174/0929867328666211111163701 (PMID: 34766886).

[28] E. Hannappel, beta-Thymosins, Ann. N. Y. Acad. Sci. 1112 (2007) 21–37, https://doi.org/10.1196/annals.1415.018.

[29] G. Sosne, P. Qiu, A.L. Goldstein, M. Wheater, Biological activities of thymosin beta4 defined by active sites in short peptide sequences, FASEB J. 24 (2010) 2144–2151, https://doi.org/10.1096/fj.09-142307.

[30] A. Kuzan, Thymosin β as an actin-binding protein with a variety of functions, Adv. Clin. Exp. Med. 25 (2016) 1331–1336, https://doi.org/10.17219/acem/32026.

[31] Y. Xing, Y. Ye, H. Zuo, Y. Li, Progress on the function and application of Thymosin β4, Front. Endocrinol. (Lausanne) 12 (2021) 767785, https://doi.org/10.3389/fendo.2021.767785.

[32] N. Kumar, P. Nakagawa, B. Janic, C.A. Romero, M.E. Worou, S.R. Monu, E. L. Peterson, J. Shaw, F. Valeriote, E.M. Ongeri, J.M. Niyitegeka, N.E. Rhaleb, O. A. Carretero, The anti-inflammatory peptide ac-SDKP is released from thymosin-β4 by renal meprin-α and prolyl oligopeptidase, Am. J. Physiol. Ren. Physiol. 310 (2016) F1026–F1034, https://doi.org/10.1152/ajprenal.00562.2015.

[33] T. Cabras, F. Iavarone, C. Martelli, D. Delfino, D.V. Rossetti, I. Inserra, B. Manconi, C. Desiderio, I. Messana, E. Hannappel, G. Faa, M. Castagnola, High-resolution mass spectrometry for thymosins detection and characterization, Expert. Opin. Biol. Ther. 15 (2015) S191–S201, https://doi.org/10.1517/14712598.2015.1009887.

[34] S.R. Van Doren, Matrix metalloproteinase interactions with collagen and elastin, Matrix Biol. 44-46 (2015) 224–231, https://doi.org/10.1016/j.matbio.2015.01.005.

[35] H. Kuivaniemi, G. Tromp, Type III collagen (COL3A1): gene and protein structure, tissue distribution, and associated diseases, Gene 707 (2019) 151–171, https://doi.org/10.1016/j.gene.2019.05.003.

[36] Y. Xing, Y. Ye, H. Zuo, Y. Li, Progress on the function and application of Thymosin β4, Front. Endocrinol. (Lausanne) 12 (2021) 767785, https://doi.org/10.3389/fendo.2021.767785.

[37] P. Qiu, M. Kurpakus-Wheater, G. Sosne, Matrix metalloproteinase activity is necessary for thymosin beta 4 promotion of epithelial cell migration, J. Cell. Physiol. 212 (2007) 165–173, https://doi.org/10.1002/jcp.21012.

[38] N.D. Rawlings, M. Waller, A.J. Barrett, A. Bateman, MEROPS: the database of proteolytic enzymes, their substrates and inhibitors, Nucleic Acids Res. 42 (2014) D503–D509, https://doi.org/10.1093/nar/gkt953.

[39] D. Wang, Y. Fu, J. Fan, Y. Wang, C. Li, Y. Xu, H. Chen, Y. Hu, H. Cao, R.C. Zhao, W. He, J. Zhang, Identification of alpha-enolase as a potential immunogenic molecule during allogeneic transplantation of human adipose-derived mesenchymal stromal cells, Cytotherapy 24 (2022) 393–404, https://doi.org/10.1016/j.jcyt.2021.10.004.

[40] T. Nakano, S. Goto, Y. Takaoka, H.P. Tseng, T. Fujimura, S. Kawamoto, K. Ono, C. L. Chen, A novel moonlight function of glyceraldehyde-3-phosphate dehydrogenase (GAPDH) for immunomodulation, Biofactors 44 (2018) 597–608, https://doi.org/10.1002/biof.1379.

[41] L.M. Yin, M. Schnoor, C.D. Jun, Structural characteristics, binding partners and related diseases of the Calponin homology (CH) domain, Front. Cell Dev. Biol. 8 (2020) 342, https://doi.org/10.3389/fcell.2020.00342.

[42] M. Kornreich, R. Avinery, E. Malka-Gibor, A. Laser-Azogui, R. Beck, Order and disorder in intermediate filament proteins, FEBS Lett. 589 (2015) 2464–2476, https://doi.org/10.1016/j.febslet.2015.07.024.

[43] N. Al-Sharabi, R. Gruber, M. Sanz, S. Mohamed-Ahmed, E.K. Kristoffersen, K. Mustafa, S. Shanbhag, Proteomic analysis of mesenchymal stromal cells Secretome in comparison to leukocyte- and platelet-rich fibrin, Int. J. Mol. Sci. 24 (2023) 13057, https://doi.org/10.3390/ijms241713057.

[44] S. Shin, J. Lee, Y. Kwon, K.S. Park, J. Jeong, S.J. Choi, S.L. Bang, J.W. Chang, C. Lee, Comparative proteomic analysis of the mesenchymal stem cells Secretome from adipose, bone marrow, placenta and wharton's jelly, Int. J. Mol. Sci. 22 (2021) 845, https://doi.org/10.3390/ijms22020845.

[45] A.O. Pires, B. Mendes-Pinheiro, F.G. Teixeira, S.I. Anjo, S. Ribeiro-Samy, E. D. Gomes, S.C. Serra, N.A. Silva, B. Manadas, N. Sousa, A.J. Salgado, Unveiling the differences of Secretome of human bone marrow mesenchymal stem cells, adipose tissue-derived stem cells, and human umbilical cord perivascular cells: a proteomic analysis, Stem Cells Dev. 25 (2016) 1073–1083, https://doi.org/10.1089/scd.2016.0048.

[46] D. Kehl, M. Generali, A. Mallone, M. Heller, A.C. Uldry, P. Cheng, B. Gantenbein, S. P. Hoerstrup, B. Weber, Proteomic analysis of human mesenchymal stromal cell secretomes: a systematic comparison of the angiogenic potential, NPJ Regen Med. 4 (2019) 8, https://doi.org/10.1038/s41536-019-0070-y.

[47] J. Li, Z. Wu, L. Zhao, Y. Liu, Y. Su, X. Gong, F. Liu, L. Zhang, The heterogeneity of mesenchymal stem cells: an important issue to be addressed in cell therapy, Stem Cell Res Ther 14 (2023) 381, https://doi.org/10.1186/s13287-023-03587-y.

[48] C. Medrano-Trochez, P. Chatterjee, P. Pradhan, H.Y. Stevens, M.E. Ogle, E. A. Botchwey, J. Kurtzberg, C. Yeago, G. Gibson, K. Roy, Single-cell RNA-seq of out-of-thaw mesenchymal stromal cells shows tissue-of-origin differences and inter-donor cell-cycle variations, Stem Cell Res Ther 12 (2021) 565, https://doi.org/10.1186/s13287-021-02627-9.

[49] J. Zhang, M.C. Reedy, Y.A. Hannun, L.M. Obeid, Inhibition of caspases inhibits the release of apoptotic bodies: Bcl-2 inhibits the initiation of formation of apoptotic

bodies in chemotherapeutic agent-induced apoptosis, J. Cell Biol. 145 (1999) 99–108, https://doi.org/10.1083/jcb.145.1.99.
[50] M. Gerwing, V. Kocman, M. Stölting, A. Helfen, M. Masthoff, J. Roth, K. Barczyk-Kahlert, L. Greune, M.A. Schmidt, W. Heindel, C. Faber, S. König, M. Wildgruber, M. Eisenblätter, Tracking of tumor cell-derived extracellular vesicles in vivo reveals a specific distribution pattern with consecutive biological effects on target sites of metastasis, Mol. Imaging Biol. 22 (2020) 1501–1510, https://doi.org/10.1007/s11307-020-01521-9.
[51] H.K. Lee, B.R. Lee, T.J. Lee, C.M. Lee, C. Li, P.M. O'Connor, Z. Dong, S.H. Kwon, Differential release of extracellular vesicle tRNA from oxidative stressed renal cells and ischemic kidneys, Sci. Rep. 12 (2022) 1646, https://doi.org/10.1038/s41598-022-05648-3.
[52] D. Sproviero, S. La Salvia, M. Giannini, V. Crippa, S. Gagliardi, S. Bernuzzi, L. Diamanti, M. Ceroni, O. Pansarasa, A. Poletti, C. Cereda, Pathological proteins are transported by extracellular vesicles of sporadic amyotrophic lateral sclerosis patients, Front. Neurosci. 12 (2018) 487, https://doi.org/10.3389/fnins.2018.00487.
[53] V. Marassi, G. La Rocca, A. Placci, A. Muntiu, F. Vincenzoni, A. Vitali, C. Desiderio, T. Maraldi, F. Beretti, E. Russo, V. Miceli, P.G. Conaldi, A. Papait, P. Romele, A. Cargnoni, A.R. Silini, F. Alviano, O. Parolini, S. Giordani, A. Zattoni, P. Reschiglian, B. Roda, Native characterization and QC profiling of human amniotic mesenchymal stromal cell vesicular fractions for secretome-based therapy, Talanta 276 (2024) 126216, https://doi.org/10.1016/j.talanta.2024.126216.
[54] J. Schira-Heinen, L. Grube, D.M. Waldera-Lupa, F. Baberg, M. Langini, O. Etemad-Parishanzadeh, G. Poschmann, K. Stuhler, Pitfalls and opportunities in the characterization of unconventionally secreted proteins by secretome analysis, Biochim. Biophys. Acta, Proteins Proteomics 1867 (2019) 140237, https://doi.org/10.1016/j.bbapap.2019.06.004.
[55] F. Pischiutta, L. Brunelli, P. Romele, A. Silini, E. Sammali, L. Paracchini, S. Marchini, L. Talamini, P. Bigini, G.B. Boncoraglio, R. Pastorelli, M.G. De Simoni, O. Parolini, E.R. Zanier, Protection of brain injury by amniotic mesenchymal stromal cell-secreted metabolites, Crit. Care Med. 44 (2016) e1118–e1131, https://doi.org/10.1097/CCM.0000000000001864.
[56] Y. Perez-Riverol, J. Bai, C. Bandla, S. Hewapathirana, D. García-Seisdedos, S. Kamatchinathan, D. Kundu, A. Prakash, A. Frericks-Zipper, M. Eisenacher, M. Walzer, S. Wang, A. Brazma, J.A. Vizcaíno, The PRIDE database resources in 2022: A hub for mass spectrometry-based proteomics evidences, Nucleic Acids Res. 50 (2022) D543–D552, https://doi.org/10.1093/nar/gkab1038.